



Cycle counting of roller bearing oscillations – case study of wind turbine individual pitching system

Matthias Stammler^{1,*}, Andreas Reuter¹ and Gerhard Poll²

¹ Fraunhofer IWES, Appelstrasse 9A, 30167 Hanover, Germany

² IMKT, Leibniz Universität Hannover, Welfengarten 1 A, 30167 Hanover, Germany

The amplitude, frequency and number of oscillating movements have a significant impact on the possible damage modes of rolling bearings. Changes in amplitude change both the fatigue and wear risk of the raceways. In order to properly calculate the fatigue lifetime of an oscillating bearing, estimate the risk of surface-induced damage modes and design test programs for such bearings, it is necessary to understand the characteristics of the oscillating movements. This paper presents a comprehensive method for the analysis of time series data including position and loads. The method is applied to the simulated time-series data of the IWT 7.5-164 reference wind turbine. Wind turbine blades typically experience wide-band dynamic loads due to stochastic wind conditions. Therefore, it is important to use time series based cycle counting methods.

Introduction

Beginning with the early works of Palmgren and Lundberg, bearings in rotating applications have been the focus of numerous research efforts [1]. Oscillating bearings, however, have not been investigated to a similar depth so far [2]. Oscillating applications are less common than rotating applications; they include those occurring unintentionally ones like vibrations of car wheel bearings during ship transport and those executed intentionally like crane head movements [3]. An increasingly important application of oscillating bearings are wind turbine blade bearings.

Blade bearings (also called pitch bearings) are large, grease-lubricated rolling bearings that connect the rotor blades and the rotor hub of pitch-controlled wind turbines. They allow turning (pitching) the blades around their primary (z-) axis, see Figure 1. Turning the blades, changes the amount of lift they generate. Thus, pitching can be used for both power and load control of the wind turbine [4].

The largest rotatory movement of a blade is a 90° turn, which is used to change from power production mode to idling or vice versa. The 0° and 90° positions in Figure 1 indicate this movement. Under most circumstances, all movements of pitch bearings are

oscillatory in nature, as the power output of the blades is at maximum at the 0° position. As the wind speed and turbulence are of complex, stochastic nature, this is also the case for the loads and movements of blade bearings.

Bossanyi presented the benefits of load reduction control mechanisms in 2003 [5]. So-called individual pitch controllers (IPC) control the pitch angle of each blade individually with the aim of harmonizing the loads of all the blades and reducing the load peaks of each individual blade. As the load reduction is substantial and the loss in power output acceptable, most turbine manufacturers use or plan to use IPC. Compared with the classical collective pitch control, IPC leads to different movement patterns of the blade bearings, with a substantial increase in small oscillations of 0.2–1.5° for an individual amplitude.

The character of the oscillations affects the risk of two possible damage modes of the bearing rings: rolling contact fatigue (RCF) and surface-induced damage modes. This is mainly driven by the formation of a lubricant film between the rolling bodies and the raceways of the bearing rings. At larger amplitudes and higher rolling speeds, the formation of a lubricant film that separates the contact bodies is more likely [6]. A separation of the contact bodies reduces the risk of surface-induced damage on the raceways.

*Corresponding author: Stammler, M. (matthias.stammler@iwes.fraunhofer.de)

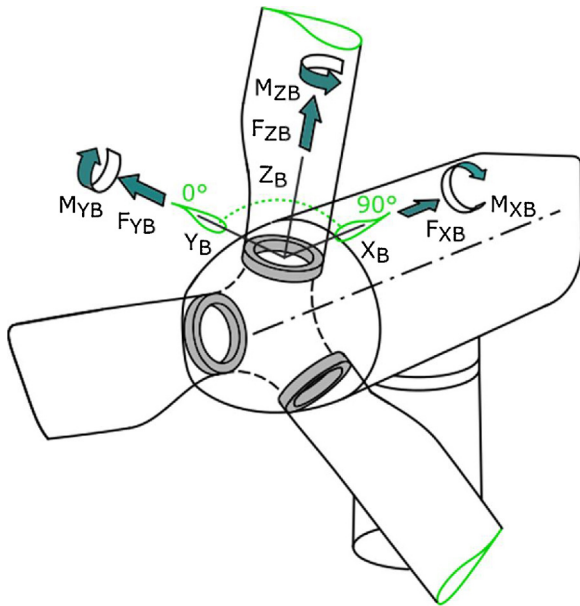


FIGURE 1

Blade coordinate system and pitch angle definition.

The most basic approach to integrate oscillations in the calculation of bearing fatigue lifetime is to sum them and convert the distance passed into full rotations, which are used for a lifetime calculations similar to the ISO281 [7,8]. Houpert and later Kotzalas and Doll presented a method to adapt fatigue lifetime calculations taking account of the oscillation angles [9,10]. Both these methods are not applicable for very small oscillation angles, as surface-induced wear is the dominating damage mode in this case. Schwack et al. [2] compare different fatigue lifetime calculation methods [2]. This comparison showed huge differences in the calculated lifetime for different approaches.

None of the aforementioned publications (except for [2]) mentions how to obtain the oscillation cycles from a given data set. Due to the widespread use of rainflow countings [11,12] for fatigue calculations, we assume this method to be the standard approach.

As part of the development process, all wind turbines are simulated in aero-elastic simulation tools like Bladed, Fast and HAWC2 according to IEC 61400 [13]. These models integrate the original pitch controller of the turbine. The movements of the pitch bearings are included within the time-series outputs of these tools. While it is also possible to measure the movements on existing turbines, it is necessary to use simulation data for the development of new turbine types, new controllers and blade modifications.

Although not the entire turbine lifetime is simulated, the amount of data created is vast and needs to be organized in order to be used as input for the subsequent development of individual components. Typical analytical methods include the abovementioned rainflow counting, the creation of load bin distributions and the calculation of damage-equivalent loads for different slopes of S-N-curves.

In this paper, the simulation data obtained with an aero-elastic model of the IWT7.5-164 reference turbine [14] is presented in 'Reference turbine IWT7.5-164 and simulation' section and used for the subsequent analysis. The following 'Effect of movements on damage modes' section briefly describes the impact of

TABLE 1

Main parameters of the IWT 7.5-164 [14].

Property	Symbol	Value
Wind class		IEC A1
Hub height	h_{hub}	119.3 m
Rotor diameter (unconed)	D_{rotor}	164 m
Cut-in wind speed	V_{in}	3 m/s
Rated wind speed	V	11 m/s
Cut-out wind speed	V_{out}	25 m/s
Minimum rotational speed	Ω_{min}	5 rpm
Rated rotational speed	Ω_r	10 rpm
Design tip speed ratio	λ_D	8.4
Rotor configuration		Upwind, 3-blade
Tower mass	m_{tower}	1,467,355 kg
Rotor-Nacelle-Assembly mass	m_{RNA}	536,586 kg
Drive train concept		Direct drive

oscillation characteristics on damage modes. Existing analytical methods for time series containing oscillating data are evaluated for the purpose of blade-bearing movement analysis in 'Analysis of oscillations' section. 'Program for data analysis' section describes a new, comprehensive method for the analysis of blade-bearing movement data based on the findings of the afore-mentioned sections. This method is applied to the simulation data of the IWT7.5-164 reference turbine and the results are presented, both in 'Results and discussion' section. The paper finishes by the conclusions in 'Conclusions' section.

Methods

Reference turbine IWT7.5-164 and simulation

The IWT7.5-164 reference turbine is a nearshore wind turbine with 164 m rotor diameter and a rated power output of 7.5 MW. Its pitch controller includes IPC-algorithms. The IPC is active at wind speeds of approximately the rated speed of 11 m/s and above [14]. Table 1 contains the most important properties of the turbine.

The design of the blade bearing has been described by Schwack et al. [15]. It is a double-row four-point-contact bearing with a pitch diameter of 4690 mm. The balls have a diameter of 80 mm. For every degree of rotational movement, the ball covers a rolling distance x of 20.1 mm on the raceway. The short axis of the Hertzian contact ellipse (2b, see Figure 4) under typical operating conditions is in the range of 4–5 mm.

A complete simulation set according to IEC 61400-1 [13] was executed in the HAWC2 simulation code [16]. The duration of each simulation was 600 s (except for start/stop and error simulations). 684 fatigue simulations were carried out. The discrete time steps of the output were 20 ms, resulting in 30,000 values per channel for each simulation file. The simulation output files in ASCII format have an overall size of 130 GB. Of the signals available, the pitch angles of the blades and the loads at the blade roots, which are the same as the blade-bearing loads, are of particular interest. Figure 2 shows one exemplary time series. The mean wind speed of this simulation is 11 m/s, which is the rated wind speed of the turbine. The movements of one of the blade bearings (signal "pitch angle") and the dominant loads on that bearing (signals "M_{yb}" and "M_{xb}", see also Figure 1) are shown. The pitch angle movements consist of small oscillations with double amplitude of up to 4° and of larger movements. The oscillations with larger

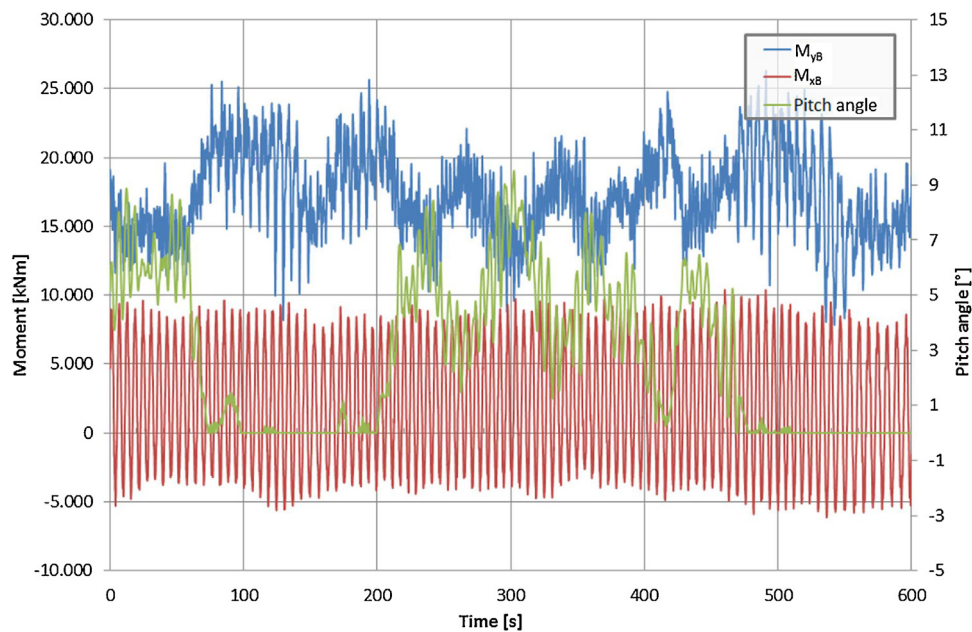


FIGURE 2

IWT7.5-164 wind turbine simulation at 11 m/s mean wind speed.

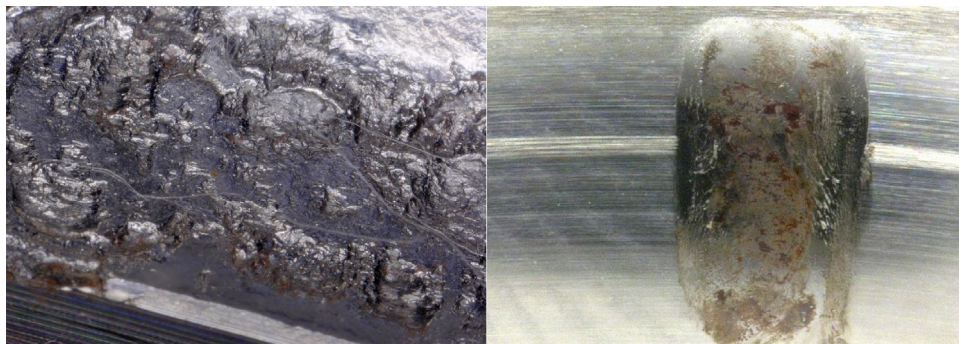


FIGURE 3

Severe fatigue damage (left) and surface-induced damage (right) on bearing raceways.

amplitudes control the power output of the turbine, whereas the turbines' IPC executes oscillations with smaller amplitudes for the purpose of load reduction.

As the simulated time of 600 s is just a short interval of the overall lifetime of the turbine, each simulation run of 600 s represents a longer period. This period is obtained by using the distribution of the wind speed over 20 years. The IWT7-5164 is designed for IEC class IA. The IEC 61400-1 [13] contains a description of the site conditions for the different generic classes and the methods for multiplying the simulation data to obtain the loads for the full lifetime.

Effect of movements on damage modes

Assuming a bearing is correctly designed and mounted, the two main damage modes of pitch bearings are rolling contact fatigue and surface-induced damage modes on the bearing raceways [6]. RCF is the dominant mode when a lubricant film separates the rolling bodies from the raceway and no metal-metal-contact occurs. Lundberg and Palmgren first described the fatigue mechanisms in rolling bearings [1], today fatigue calculation is

standardized in the ISO 281 [8]. This is the case for long, steady rotations with relatively high speed, when elasto-hydrodynamic conditions apply. The extent of RCF damage is affected, among others things, by the number of times a rolling body passes a certain area of the raceway and by the load [17]. The left part of Figure 3 shows severe RCF damage on the raceway of a four-point contact bearing.

Oscillations with small amplitudes, however, give rise to surface-induced damage. Elasto-hydrodynamic contact conditions are less likely than mixed lubrication regimes. Surface-induced damage might appear in the form of False Brinelling and/or Fretting Corrosion [18]. The right part of Figure 3 shows surface-induced damage on the raceway of a four-point-contact bearing.

The risk of it occurring, its severity and the speed of damage progression depend on several parameters. These are, among others, the amplitude and speed of the oscillations, the load and lubricant. Whether an oscillation generates surface-induced damage also depends on the size of the contact patch between the rolling body and raceway as well as the size of the bearing. Thus, amplitudes of different bearings should not be compared by means

of their absolute value in degrees, but rather by the relation between the rolling distance x and the size of the contact patch along this direction $2b$ (see Figure 4).

This relation is also called the amplitude ratio. The findings of Maruyama and Saitoh for oil-lubricated bearings [19] are used for the subsequent analysis: In [19], it is shown that an amplitude ratio of 1.5 is necessary to build up a lubricant film in an oil-lubricated contact. This ratio is likely to differ with grease-lubricated bearings, and the difference depends on several parameters. Grease is composed of thickener (soap) and base oil, and the base oil forms the lubricant film under most conditions. As the oil is contained in the thickener matrix and the proportion which leaves this matrix is limited, oil supply to the rolling contact is limited as well and lubricant film thickness is lower than in purely oil-lubricated bearings under most conditions. However, thickener is also able to enter the contact area, and in such a case, it contributes to the separation of the contact partners. Thus, the above-mentioned value is taken as an indication for the risk of surface-induced damage.

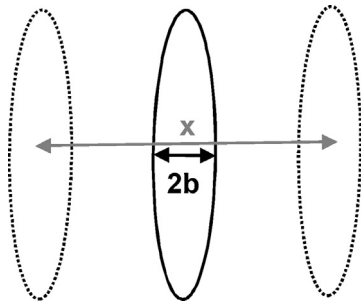


FIGURE 4
 $x/2b$ dimensionless distance parameter.

Analysis of oscillations

As the size of the output files of the simulation makes it inefficient to use them as a direct input for component design calculation, the data have to be processed prior to further design steps. The results of this processing are used to calculate the fatigue lifetime of an oscillating bearing, estimate the risk of surface-induced damage modes and design test programs for such bearings.

Common analytical methods include rainflow counting [12], bin counting of signals and damage equivalent load calculation [20]. Figure 5 outlines the different approaches of these three methods, the following figures show detailed views of the individual processes. The left part of Figure 5 shows the process of rainflow counting. The result of a rainflow count is a sorted matrix containing different classes of amplitudes and the respective numbers of cycles. The middle part of Figure 5 visualizes the bin-counting algorithm. This algorithm delivers the total duration a signal is within a certain range of values. If the number of bearing rotations is counted as well, the bin counting results in a so-called Load Revolution Distribution (LRD, not included in Figure 5). The right part of Figure 6 shows an additional simplification of the rainflow counting result, the damage equivalent loads (DEL). For a fixed number of cycles and a given S/N slope, DEL give the amplitude of oscillations whose damage matches the damage of the rainflow counting result.

Rainflow counting is widely used to create data input for fatigue calculations (see the left side of Figure 6). The algorithm treats the distance between the minimum and the maximum value as a single flank or half cycle (see number 1 in Figure 6). The name rainflow count is derived from this interpretation, as the red path behaves like a water drop flowing down a roof if the figure is turned through 90°. To avoid double counting of value changes, other flanks that would interfere with the way of the red path are intersected by it. This thus creates cycles 2/3, 4/5 and 6/7. The

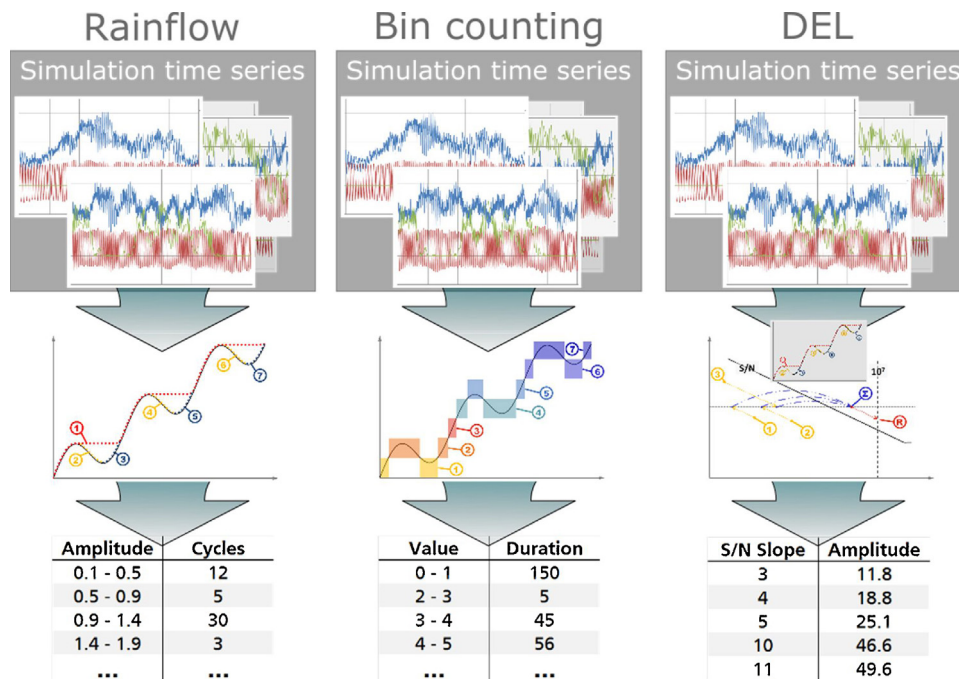


FIGURE 5
 Analytical methods: rainflow counting, bin counting, damage equivalent loads.

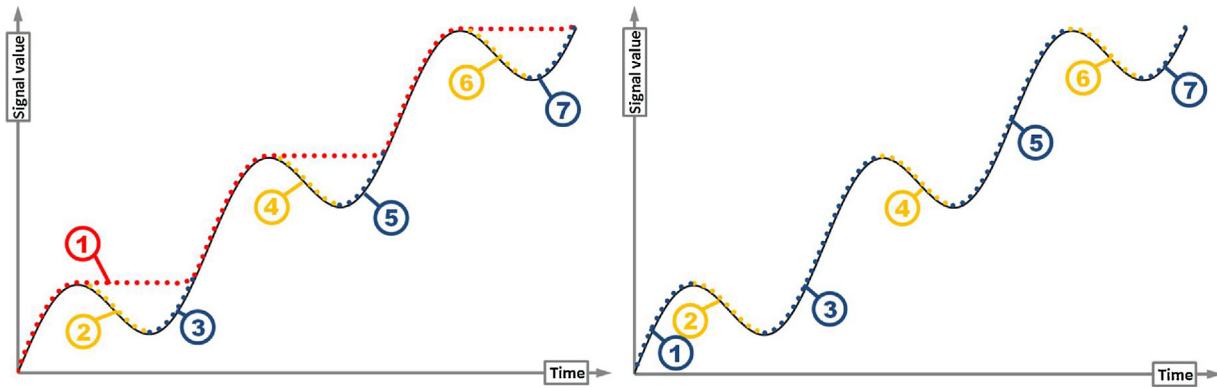


FIGURE 6

Rainflow counting (left) vs. range pair counting (right).

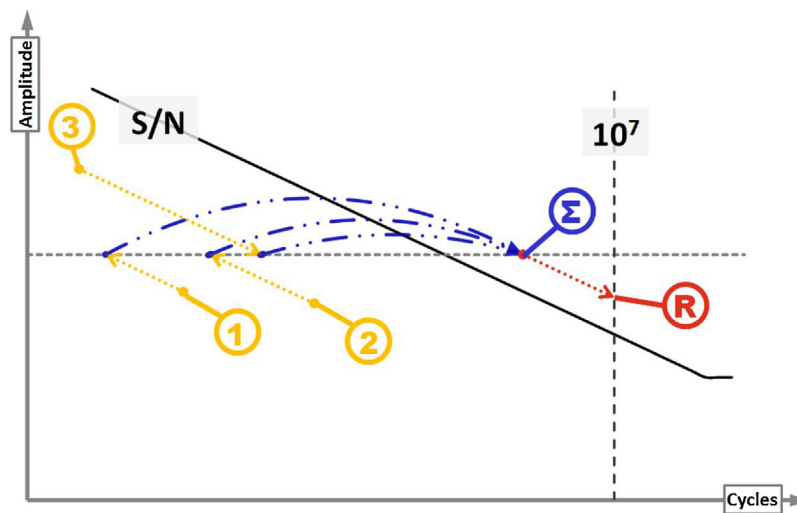


FIGURE 7

Damage equivalent load process.

half cycle 1 is relevant for the structural fatigue damage of materials (see [12] for further details). However, with regard to blade-bearing movements, it is more important to focus on the single distances x covered by the roller/ball on the raceway. Every interruption of a movement leads to a breakdown of possible lubricant films and has to be taken into account. As such, the less common range-pair counting approach (see the right side of Figure 6) is more suitable in this case. Rainflow counting overestimates the number and amplitude of long cycles (see 1 in Figure 6) and the number of cycles with relatively small amplitudes (see 3, 5 and 7 in Figure 6).

In its most basic form, bin counting provides the period of time that any given signal spends within a set range of values. Combinations of bins, for example, subsequent counting of second signal values may be used to obtain more information. As no amplitude information is stored, bin counting as a solitary tool is not valuable in the analysis of blade-bearing movements. Yet, applying bin counting as a supplementary method to the range-pair counting is beneficial, as the combination of the two gives information on the load level for certain oscillating movements, for example.

The process of DEL creation is also shown in Figure 7. The results of the rainflow counting are a number of combinations of

amplitudes and cycles (indicated as 1, 2, 3 in the figure). Given a certain S/N slope, these values are transferred to an arbitrarily chosen amplitude level that is the same for all values (dotted arrows in Figure 7). The cycle values can then be summed (Σ -symbol in Figure 7). The S/N slope is again used to transfer this summed value to a chosen number of cycles and the corresponding amplitude level. None of these operations changes the summed fatigue damage to the part. As any information about single amplitude values is erased in the process, DEL results are not suitable for the analysis of blade-bearing movements.

Program for data analysis

To take account of the range-pair counting method and additional bin counting, a MATLAB-program was created for the purpose of blade-bearing movement and load analysis. Figure 8 shows a flow chart of this program. The raw time series data is used as the input. The blade pitch angle signal is analyzed by a range-pair counting algorithm which includes an evaluation of the mean value of each half cycle. For each half cycle, additional signals like MxB or MyB are taken into account via a bin-counting algorithm.

Figure 9 shows an exemplary time series and visualizes the results of the analysis. The time series file chosen for this example

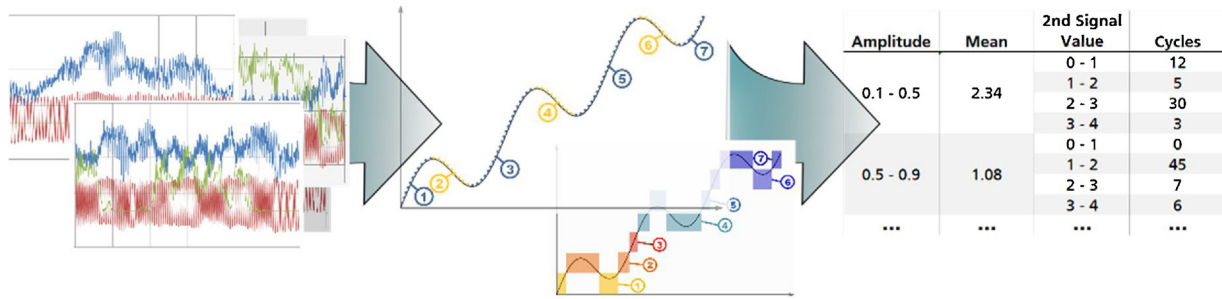


FIGURE 8
 MATLAB program: simulation time series (left) are processed via range-pair and bin counting into a result matrix.

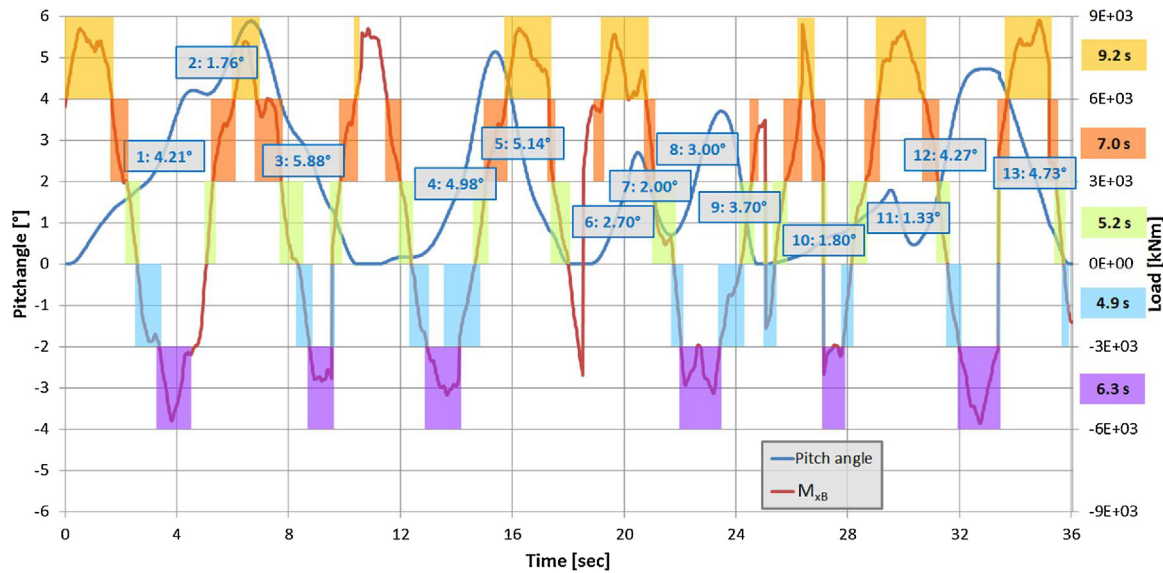


FIGURE 9
 Visualization of the analytical results of an exemplary time series.

was one of the six files (seeds) of DLC1.1 with a wind speed of 9 m/s and the wind direction of 0°. The pitch angle signal is shown in blue and contains 13 visually identified half cycles with double amplitude above 1°. This threshold was set arbitrarily to allow easy visual identification. The amplitude sizes (in the gray boxes of Figure 9) are the output of the MATLAB-analysis. The bin counting result of M_{xB} (red signal) is visually interpreted by means of colored boxes. The bin counting is executed only when pitch half-cycles are identified. Time periods without colored boxes are such periods where no half cycles were identified (either standstill or too small an amplitude).

Results and discussion

All fatigue load cases according to IEC 61400-1 [13] were analyzed, namely the Design Load Cases 1.2, 2.4, 3.1, 4.1 and 6.4. The operating time of these load cases sums up to 175,000 h, that is, approx. 20 years. Start and stop (DLC 3.1 and 4.1) were assumed to occur 1100 times each year based on values of comparable wind turbines.

Table 2 shows the results of a range-pair counting of movements between 0.03° and 90° width. The lower value is included in the range, the upper excluded. The overall number of cycles identified is 566×10^7 . Taking the mean frequency and the numbers of cycle, it can be calculated that the pitch system is active for 35% of the

operating time or 60,766 h. This figure corresponds to the IPC controller mode being active at the rated speed and above, as the Weibull distribution for this wind class implies a probability of 37% for wind speeds of 10 m/s and above. The high number of cycles in the smallest amplitude bin (0.03–5°) is typical for an individual pitch controlled turbine as well.

As most pitch activity occurs in the bin with the smallest amplitudes (0.03–5° in Table 2), it is further split up into finer bins, see Table 3. The amplitude is given both in degrees and rolling distance covered by the ball on the raceway. Assuming an amplitude ratio of roughly 1.5 as the lower limit for a lubricant film formation (cf. ‘Effect of movements on damage modes’ section), a limit for cycles that impose a risk of surface-induced damage can be estimated. This limit is only an orientation value, as further research in the field of oscillating movements of grease-lubricated contacts is necessary. A value of 0.4° for the double amplitude was chosen as it was closest to an amplitude ratio of 1.5. The sum of all cycles with amplitudes equal to or smaller than 0.4° is 1.29×10^7 . In several research projects dealing with smaller oscillating bearings, surface-induced damage was created with far lower cycle numbers of up to 0.5×10^6 . A list of research projects and the kinematic conditions investigated in these can be found in [6]. Thus, the results confirm that there is a risk of surface-induced damage in the investigated case.

TABLE 2

Cycle count results for 0–90°.

Double amplitude (°)	Number of full cycles (-)	Mean frequency (Hz)
0.03–5	4.81E + 07	0.43
5–10	8.11E + 06	0.16
10–15	3.31E + 05	0.11
15–20	1.97E + 04	0.10
20–25	1.15E + 03	0.05
25–30	4.79E + 03	0.03
30–90	1.76E + 04	0.02

TABLE 3

Detailed cycle count results for 0–5°.

Double amplitude (°)	Double amplitude x (mm)	Number of full cycles (-)	Mean frequency (Hz)
0.03–0.2	0.6–4	8.66E + 06	0.87
0.2–0.4	4–8	4.25E + 06	0.59
0.4–0.6	8–12.1	3.05E + 06	0.51
0.6–0.8	12.1–16.1	2.32E + 06	0.45
0.8–1.0	16.1–20.1	2.30E + 06	0.40
1.0–1.2	20.1–24.1	2.00E + 06	0.37
1.2–1.4	24.1–28.2	1.84E + 06	0.33
1.4–1.6	28.2–32.2	1.63E + 06	0.31
1.6–1.8	32.2–36.2	1.73E + 06	0.30
1.8–2.0	36.2–40.2	1.43E + 06	0.28
2.0–3.0	40.2–60.3	6.37E + 06	0.25
3.0–4.0	60.3–80.5	6.76E + 06	0.21
4.0–5.0	80.5–100.6	5.77E + 06	0.19

TABLE 4

Bin count of pitch angle mean values.

Double amplitude (°)	Pitch angle value (°)	Operational time (h)
0.03–0.40	0–2.5°	3450.47
	2.5–5°	289.81
	5–10°	658.67
	10–15°	553.69
	15–20°	198.00
	20–25°	45.27
0.40–1.00	0–2.5°	2979.88
	2.5–5°	534.41
	5–10°	964.93
	10–15°	720.15
	15–20°	310.73
	20–25°	64.01
1.00–5.00	0–2.5°	6208.65
	2.5–5°	3950.09
	5–10°	9480.14
	10–15°	9417.40
	15–20°	4595.34
	20–25°	1290.96

A high number of oscillations with small amplitudes increases the risk of surface-induced damage, especially if the mean values do not change over time. A changing mean value would result in a change of the raceway areas that are in contact with the rolling bodies. These areas share the oscillations/loads, thus reducing the probability that one individual area will fail. To better understand the mean value behavior of the pitch angle, a bin count of the pitch angle was performed in addition to the range pair count.

TABLE 5

Bin count of resulting bending moment.

Double amplitude (°)	Resulting bending moment (kNm)	Operational time (h)
0.03–0.40	6000–8000	135
	8000–10,000	205
	10,000–12,000	286
	12,000–14,000	401
	14,000–16,000	601
	16,000–18,000	928
	18,000–20,000	1116
	20,000–22,000	924
	22,000–24,000	452
24,000–26,000	106	

Table 4 shows the results of this bin count. For double amplitudes smaller than 0.4°, 66% of the oscillations have a mean value between 0 and 2.5°. This range contains the largest single operating time bin in the evaluated values. Sixty-six percent equals 0.86×10^7 cycles, a number still high enough to impose a risk of surface-induced damage.

The analysis of pitch angle amplitudes indicates the risk of surface induced damage for this blade bearing. Whether such damage occurs also depends on various other factors, one of them being the applied load. To gain an understanding of the load conditions, a bin count of the resulting bending moment was carried out. Table 5 contains the results of this bin counting.

The analytical result is a range pair count including oscillation frequencies and accompanying bin count of pitch angle and

bending moments. This result can be used as input for a rolling contact fatigue calculation (see [2]) or to design a test program for either a test of surface-induced damage modes or rolling contact fatigue. For fatigue calculations, it is recommended to use a higher number of load bins, as otherwise the design of the bearing would be too conservative [21]. The MATLAB-program we use for this paper can easily extract smaller bin sizes, yet the length of a table containing several hundreds of bins is too large for the format of this paper. High bin numbers are not necessarily needed for estimations on the probability of surface-induced damage modes. The dependence of such damage modes on outer load has not been put into calculation methods so far.

Conclusions

Rolling bearings in oscillatory applications may be subject to different damage modes than bearings in rotating applications. To better understand the nature of the damage mechanisms of such bearings, it is necessary to describe the oscillatory movements. In this paper different methods of analyzing movement data of oscillating bearings were presented. The blade bearings of the IWT7.5-164 reference wind turbine were used as an example to demonstrate the methods. The possible damage modes of raceways were briefly presented and the amplitude ratio $x/2b$ was used instead of absolute amplitudes for further analysis. It was shown that rainflow counting is not a suitable method to analyze movement data, as rainflow counts overestimate the number of both very small and very large amplitude cycles. A combination of range pair counting and bin counting was applied to the output data of the aeroelastic simulations of the reference wind turbine. Taking account of amplitude ratios that most likely will not allow for lubricant film formation ($x/2b < 1.5$), it was found that cycles with a double amplitude of 0.4° or less bear a risk that surface-induced damage modes will occur. 0.4° is equivalent to a distance of approx. 8 mm on the raceways. 1.29×10^7 cycles with such amplitudes were identified. In a second step, a bin count of the pitch angle values showed that 0.86×10^7 or 66% of the aforementioned cycles are movements around a middle position in the range of $0\text{--}2.5^\circ$. If these cycles were in a direct succession, it would have a duration of approx. 127 days. Furthermore, a bin count of the resulting bending moments showed that 58% of the bending moments are within a range of 16–22 MNm. A risk of surface-induced damage was identified. The results of the analysis can be used for RCF calculations or to design test programs for different damage modes.

Future work in this field will aim at a better understanding of the risk of surface-induced damage for a given bearing system. Part of

this work will be a movement pattern analysis of data and incorporation of long term wind measurements. Advanced pattern recognition, in particular, will allow for a better understanding of critical conditions. The work will also include bearing tests under different oscillating movements to identify critical amplitude ratios under these conditions.

Conflict of interest

None declared.

Acknowledgements

The present work was carried out with the project “HAPT – Highly Accelerated Pitch Bearing Tests”. The project funding by the German Federal Ministry for Economic Affairs and Energy is kindly acknowledged.

References

- [1] G. Lundberg, A. Palmgren, *Dynamic Capacity of Rolling Bearings*, Generalstabens Litografiska Anstalts Förl., Stockholm, 1947.
- [2] F. Schwack, M. Stammer, G. Poll, A. Reuter, *J. Phys.: Conf. Ser.* 753 (2016).
- [3] J.O. Almen, *J. Mech. Eng.* (1937) 415–422.
- [4] T. Burton, *Wind Energy Handbook*, 2nd ed., Wiley, Chichester, New York, 2011.
- [5] E.A. Bossanyi, *Wind Energy* 6 (2) (2003) 119–128.
- [6] M. Stammer, G. Poll, *Schadensmechanismen in Rotorblattlagern*, 2014 Göttingen.
- [7] Germanischer Lloyd, *Richtlinie für die Zertifizierung von Windenergieanlagen*, Hamburg, 2010.
- [8] DIN ISO, *Wälzlager – Dynamische Tragzahlen und nominelle Lebensdauer (ISO 281:2007)*, Beuth, Berlin, 2010.
- [9] L. Houper, *Tribol. Trans.* 42 (1) (1999) 136–143.
- [10] M.N. Kotzalas, G.L. Doll, *Philos. Trans. R. Soc. A: Math. Phys. Eng. Sci.* 368 (1929) (2010) 4829–4850.
- [11] C.H. McInnes, P.A. Meehan, *Int. J. Fatigue* 30 (3) (2008) 547–559.
- [12] M. Matsuishi, T. Endo, *Fatigue of Metals Subjected to Varying Stress*, 1968 Fukuoka, Japan.
- [13] IEC, *Wind Turbines – Part 1: Design Requirements*, 3rd ed., International Electrotechnical Commission, Geneva, 2005.
- [14] A. Sevinc, M. Rosemeier, M. Bätge, R. Braun, F. Meng, M. Shan, D. Horte, C. Balzani, A. Reuter, *IWES Wind Turbine IWT-7.5-164*, 2014 Hannover.
- [15] F. Schwack, M. Stammer, H. Flory, G. Poll, *Free Contact Angles in Pitch Bearings and their Impact on Contact and Stress Conditions*, in: *Wind Europe Conference*, Hamburg, 2016.
- [16] T.J. Larsen, A.M. Hansen, *How 2 HAWC2, The User's Manual*, Risø National Laboratory, Roskilde, 2015.
- [17] E. Ioannides, T.A. Harris, *J. Tribol.* 107 (3) (1985) 367.
- [18] R. Errichello, *Tribol. Lubr. Technol.* 60 (2004) 34–36.
- [19] T. Maruyama, T. Saitoh, *Tribol. Int.* 43 (8) (2010) 1279–1286.
- [20] H.B. Hendriks, B.H. Bulder, *Fatigue Equivalent Load Cycle Method: A General Method to Compare the Fatigue Loading of Different Load Spectrums*, 1995.
- [21] A.R. Nejad, Z. Gao, T. Moan, *Int. J. Fatigue* 61 (2014) 116–128.